

Correlation energies of Be-like atoms: A multimodel space many-body perturbation calculation with finite basis sets

Jinhua Xi

*Laboratory of Magnetic Resonance and Atomic and Molecular Physics, Wuhan Institute of Physics,
The Chinese Academy of Sciences, P.O. Box 71010, Wuhan 430071, People's Republic of China*

Lijin Wu and Baiwen Li

*Chinese Center of Advanced Science and Technology (World Laboratory), P.O. Box 8730, Beijing 100080, People's Republic of China
and Wuhan Institute of Physics, The Chinese Academy of Sciences, P.O. Box 71010, Wuhan 430071, People's Republic of China*

(Received 10 August 1992)

With finite basis sets constructed from B splines, a systematical many-body perturbation calculation of the Be-like atoms with Z from 3 to 36 is performed. A two-configuration model space $(2s + 2p)^2$ is adopted in the calculation in order to speed the perturbation convergence. With perturbations up to the second order, we obtain 93–99.8 % of the total correlation energies given by Davidson *et al.* [Phys. Rev. A **44**, 7071 (1991)] for Z from 4 to 20. The discrepancies between experimental and theoretical values approach a constant of 0.0005 while atomic number Z increases.

PACS number(s): 31.20.Tz, 31.20.Di

I. INTRODUCTION

Many-body perturbation theory (MBPT) has been used extensively in the calculations of atomic problems, such as electron correlations, hyperfine interactions, photoionizations, etc. Two approaches are mainly used for numerical treatment. The first one, employed originally by Kelly [1] and Chang, Pu, and Das [2], is the order-by-order expansion of the perturbation Hamiltonian with the aid of basis sets. In this method, the expansion for higher orders will lead to large numbers of Goldstone diagrams, and the calculation becomes very complicated and time consuming. The continuum-orbital basis also complicates the procedure. The other approach is the coupled-cluster method, which is widely used by the group at Chalmers University of Technology (see, for example, Lindgren [3] and references therein). In this approach, one must solve a set of coupled differential equations, which may endure the problem of numerical stability. Solving two-body equations also requires a large amount of computer memory. Practical methods are available to eliminate the complexity of the basis expansion calculations. For example, recurrence relations of Goldstone diagrams can be used to include higher-order perturbation effects. In our treatment of the hyperfine interactions of the $3d$ -shell atoms, the polarization diagrams were included to all orders [4,5] by using a recurrence formula. Finite basis sets can be adopted to replace the traditionally used complete bound-continuum ones [6,7]. In recent years, the attempt to construct finite basis sets with B splines has achieved great success. The B -spline technique was originally employed by Johnson and co-workers [8,9] and Fischer and co-workers [10–12], and later by Chang [13] and Chang and Tang [14]. We developed programs to investigate the hyperfine

interaction [15], electron correlation [16], and the behavior of the hydrogen atom in superstrong magnetic fields [17,18] by using B splines, and have obtained very good results. Another practical way of avoiding complexity is to perform the MBPT calculations to the lower orders under multimodel space.

The correlation energies of the ground state of Be-like atomic ions have been analyzed by various methods [19–21]. Recently, Davidson *et al.* analyzed the ground-state experimental energies of some atomic ions and obtained improved correlation energies [22], including those of the Be-isoelectric sequence with Z from 4 to 20. The purpose of the present paper is to check the efficiency of the multimodel space MBPT calculations, provide further illustration of the application of B -spline finite basis sets, and give a systematical study of the correlation energies of the Be-like ions by presenting the results of the second-order MBPT calculations under the $(2s + 2p)^2$ two-dimensional model space with finite basis sets constructed from B splines.

II. THEORETICAL METHODS

Detailed descriptions of the properties of B splines can be found in the book of deBoor [23]. Methods of constructing finite bases with B splines were given in the papers referred to above. Here we give a brief illustration of the construction of the nonrelativistic finite basis sets.

Under the central-field approximation, the single-particle radial Hartree-Fock (HF) equation is

$$\left[\frac{d^2}{dr^2} + \frac{2}{r} [Z - Y_a(r)] - \frac{l(l+1)}{r^2} \right] P_a(r) - \frac{2}{r} X_a(r) = \epsilon_a P_a(r), \quad (1)$$

where $Y_a(r)$ and $X_a(r)$ are the direct and the exchange potential, respectively. In the following calculation, the potentials are taken to be the $1s^2$ core Hartree-Fock potentials for the convenience of the MBPT calculations.

With a set of N B splines defined on a suitably chosen knot sequence in the region $r \in [0, R_{\max}]$, and by incorporating the boundary conditions of the orbital functions, we can expand $P_a(r)$ as

$$P_a(r) = \sum_{j=2}^{N-1} C_j B_j(r), \quad (2)$$

where the first and the last B splines are eliminated by using the boundary conditions.

The exchange potential $X_a(r)$ contains the orbital function $P_a(r)$ and thus should also be expanded

$$X_a(r) = \sum_{j=2}^{N-1} C_j \bar{X}_j^a(r). \quad (3)$$

Substituting Eqs. (2) and (3) into Eq. (1), multiplying $B_i(r)$ to each side, and integrating from 0 to R_{\max} with respect to r , we get the following matrix equation:

$$\sum_j \mathcal{H}_{ij} C_j = \epsilon_a \sum_j \mathcal{B}_{ij} C_j. \quad (4)$$

Diagonalizing Eq. (4), we get a set of orbitals $\{P(r)\}$ for a given angular momentum l . These orbitals function only in the region $r \in [0, R_{\max}]$, and form an orthogonal and nearly complete basis set. In our calculation, the cutoff radius R_{\max} is taken to be the radius of the valence $2p$ orbital.

MBPT calculations can be performed with the above basis sets. For the case of ground states of Be-like atoms, the orbital energies of $2s$ and $2p$ are nearly degenerate, and MBPT calculations with single-model space will result in slow convergence. It will be much more preferable to carry out the calculation under multimodel space, including the $2s^2 1S$ and $2p^2 1S$ configurations. In this case, the total energy of the system is obtained by diagonalizing the following 2×2 matrix:

$$\mathcal{H} = \begin{pmatrix} \langle 2s^2 1S | H_{\text{eff}} | 2s^2 1S \rangle & \langle 2s^2 1S | H_{\text{eff}} | 2p^2 1S \rangle \\ \langle 2p^2 1S | H_{\text{eff}} | 2s^2 1S \rangle & \langle 2p^2 1S | H_{\text{eff}} | 2p^2 1S \rangle \end{pmatrix}, \quad (5)$$

TABLE I. Orbital energies and Slater integrals of core and valence orbitals contributed to the zero- and first-order energies (in a.u.).

Z	ϵ_{1s}	ϵ_{2s}	ϵ_{2p}	$F^0(1s, 1s)$	$F^0(2s, 2s)$	$F^0(2p, 2p)$	$F^2(2p, 2p)$	$G^1(2s, 2p)$
3	-2.792 364 4	-0.196 304 3	-0.128 636 7	1.651 686 4	0.233 975 2	0.189 511 4	0.090 199 2	0.132 006 5
4	-5.667 115 6	-0.666 064 7	-0.519 408 5	2.277 068 3	0.396 424 9	0.383 522 5	0.182 313 6	0.249 086 3
5	-9.541 978 5	-1.389 700 5	-1.167 150 2	2.902 277 6	0.551 916 5	0.573 508 4	0.273 308 2	0.350 388 9
6	-14.416 891 7	-2.364 790 5	-2.068 188 9	3.527 409 6	0.705 136 4	0.760 687 1	0.363 344 3	0.445 637 9
7	-20.291 831 6	-3.590 590 8	-3.220 975 5	4.152 500 6	0.857 328 2	0.946 197 9	0.452 769 1	0.538 117 1
8	-27.166 787 8	-5.066 792 7	-4.624 789 6	4.777 567 1	1.008 966 7	1.130 677 1	0.541 801 6	0.629 126 5
9	-35.041 754 3	-6.793 244 1	-6.279 255 9	5.402 617 7	1.160 273 3	1.314 482 3	0.630 571 9	0.719 269 3
10	-43.916 727 9	-8.769 861 3	-8.184 161 7	6.027 657 7	1.311 364 9	1.497 825 8	0.719 159 6	0.808 860 3
11	-53.791 706 2	-10.996 593 6	-10.339 376 4	6.652 690 5	1.462 309 8	1.680 804 3	0.807 615 7	0.898 079 0
12	-64.666 688 3	-13.473 410 3	-12.744 817 8	7.277 717 4	1.613 149 3	1.863 611 8	0.895 973 9	0.987 035 2
13	-76.541 673 0	-16.200 289 9	-15.400 429 3	7.902 740 3	1.763 911 2	2.046 199 7	0.984 257 4	1.075 799 3
14	-89.416 660 4	-19.177 218 4	-18.306 173 1	8.527 759 3	1.914 613 4	2.228 644 4	1.072 482 8	1.164 418 9
15	-103.291 649 6	-22.404 185 0	-21.462 020 3	9.152 775 7	2.065 269 6	2.410 976 3	1.160 661 9	1.252 927 0
16	-118.166 640 2	-25.881 182 0	-24.867 950 7	9.777 789 9	2.215 889 2	2.593 217 7	1.248 803 8	1.341 347 3
17	-134.041 631 8	-29.608 203 8	-28.523 948 4	10.402 802 4	2.366 479 4	2.775 385 0	1.336 915 1	1.429 697 2
18	-150.916 624 5	-33.585 245 9	-32.430 002 0	11.027 813 5	2.517 045 4	2.957 491 3	1.452 001 2	1.517 989 8
19	-168.791 617 9	-37.812 304 9	-36.586 101 9	11.652 823 4	2.667 591 4	3.139 546 5	1.513 066 0	1.606 235 3
20	-187.666 612 1	-42.289 378 3	-40.992 241 1	12.277 832 2	2.818 120 7	3.321 558 6	1.601 112 9	1.694 441 4
21	-207.541 606 8	-47.016 463 8	-45.648 413 6	12.902 840 2	2.968 635 7	3.503 533 9	1.689 144 5	1.782 614 4
22	-228.416 602 0	-51.993 559 8	-50.554 614 7	13.527 847 4	3.119 138 7	3.685 477 7	1.777 163 0	1.870 759 1
23	-250.291 597 6	-57.220 664 6	-55.710 840 4	14.152 854 0	3.269 631 2	3.867 394 1	1.865 170 0	1.958 879 7
24	-273.166 593 6	-62.697 777 3	-61.117 087 7	14.777 860 0	3.420 114 7	4.049 286 9	1.953 167 1	2.046 979 3
25	-297.041 590 0	-68.424 896 8	-66.773 353 8	15.402 865 6	3.570 590 3	4.231 158 7	2.041 155 5	2.135 060 9
26	-321.916 586 6	-74.402 022 4	-72.679 636 5	16.027 870 7	3.721 058 9	4.413 012 3	2.129 136 2	2.223 126 5
27	-347.791 583 5	-80.629 153 3	-78.835 933 8	16.652 875 4	3.871 521 5	4.594 849 6	2.217 110 0	2.311 178 1
28	-374.666 580 5	-87.106 288 9	-85.242 244 2	17.277 879 8	4.021 978 6	4.776 672 4	2.305 077 8	2.399 217 3
29	-402.541 577 9	-93.833 428 7	-91.898 566 1	17.902 883 8	4.172 430 9	4.958 482 3	2.393 040 2	2.487 245 5
30	-431.416 575 4	-100.810 572 4	-98.804 898 6	18.527 887 6	4.322 878 9	5.140 280 6	2.480 997 6	2.575 263 9
31	-461.291 573 1	-108.037 719 4	-105.961 240 5	19.152 891 2	4.473 323 0	5.322 068 4	2.568 950 7	2.663 273 5
32	-492.166 570 9	-115.514 869 5	-113.367 540 8	19.777 894 5	4.623 763 6	5.503 846 8	2.656 899 8	2.751 275 1
33	-524.041 568 8	-123.242 022 4	-121.023 948 8	20.402 897 6	4.774 201 0	5.685 616 7	2.744 845 3	2.839 269 6
34	-556.916 565 5	-131.219 175 9	-128.930 311 7	21.027 902 1	4.924 637 1	5.867 380 3	2.832 787 4	2.927 257 6
35	-590.791 563 7	-139.446 333 7	-137.086 683 2	21.652 904 8	5.075 069 1	6.049 135 3	2.920 726 6	3.015 239 7
36	-625.666 562 0	-147.923 493 5	-145.493 060 5	22.277 907 4	5.225 498 6	6.230 883 7	3.008 663 1	3.103 216 4

where H_{eff} is the effective Hamiltonian of the system.

The wave function of the ground state is approximated by the mixing of the wave functions of the two configurations; that is,

$$\Psi_0 = C_{2s} |2s^2 1S\rangle + C_{2p} |2p^2 1S\rangle. \quad (6)$$

The coefficients C_{2s} and C_{2p} are the weight factors of the two configurations.

Each value of the four matrix elements in Eq. (5) can be obtained order by order by using the Rayleigh-Schrödinger perturbation theory and the Goldstone diagrammatic method. The procedure is the same as that of the single-model space calculation, except that the $2s$ and $2p$ orbitals are both treated as valence orbitals and the $1s$ orbital serves as the only core orbital. Detailed illustrations of this method were given by Lindgren and Morrison [24].

III. RESULTS AND DISCUSSIONS

With the $1s^2$ core HF potential as the central-field potential, we get a set of finite bases containing all orbitals with angular momentum $l=0,1,2,\dots,7$. The B splines are of number $N=30$ and order $K=7$. Perturbations up to second order are obtained for the Be-isoelectric sequence with atomic number Z from 3 to 36. The zero- and first-order results are determined by the characteristic of the core and valence orbitals. Values of orbital energies and Slater integrals that contribute to the zero- and first-order energies are listed in Table I. The second-order energies are presented by the Goldstone diagrams, as illustrated in Fig. 1, where (a) and (b) represent the zero-body part, (c)–(f) are the one-body diagrams, and (g)–(l) give the contribution of the two-body excitation. Results for each diagram are listed in Table II. The energies converge very quickly with angular momentum l , and contributions for $l > 7$ are extrapolated by using the l^{-n} rule, with the value of n lying between 3.6 and 4.2.

From Table II, we can see that the values of the Goldstone diagrams exhibit different Z -dependent features for small and middle Z values, but all approach relatively stable values for large Z . Among these diagrams, the largest contribution comes from the zero-body diagrams Figs. 1(a) and 1(b), whose values are quite stable in the whole region of Z , and the two-body diagram Fig. 1(g), whose energy dependence on Z is quite flat for diagonal matrix elements but is strong for off-diagonal elements in the low- Z region. The contribution of the one-body diagrams, Figs. 1(c) and 1(d), is small for small Z , increases rapidly with the increasing of Z , and becomes stable for large Z .

Summarizing Tables I and II, we obtain the total results for each of the four matrix elements in Eq. (5). Diagonalizing the matrix, we list in Table III the ground-state energies for the isoelectric sequence of Be. The corresponding HF values are listed in the second column. In the third and fourth columns we list, respectively, the ground-state energies of the present MBPT calculations and the weight factors C_{2s} for the $2s^2 1S$ configuration. The factors for the $2p^2 1S$ configuration can be derived by using the normalization requirement. The correlation en-

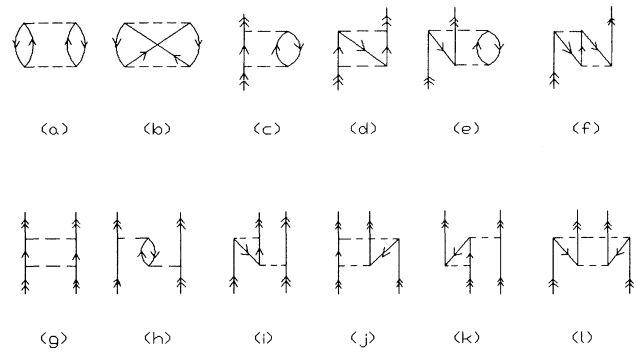


FIG. 1. Second-order correlation diagrams, where (a) and (b) represent the zero-body contributions, (c)–(f) are the one-body diagrams, and (g)–(l) give two-body excitations.

ergies are derived from the total and HF energies, and the results, together with the experimental ones of Sims *et al.* [25] and Davidson *et al.* [22], are included in the fifth and sixth columns, respectively. We can see that the second-order two-configuration MBPT results are very close to the corresponding experimental values. Compared with the single-model space MBPT calculation, the two-configuration model space formalism truly accelerates the perturbation convergence. For the Be atom, for example, the present calculation obtained 93% of the correlation energy, whereas the corresponding single-model space calculation only gains about 80% of the correlation. The agreement is even better for atoms with higher Z , and 99% of the total correlation energy has been produced for $Z > 5$. The complete agreement with the coupled-cluster calculation of Salomonson, Lindgren, and Martensson [26] for Be and C^{2+} also indicates the accuracy of the finite basis sets constructed from B splines.

It is shown from Table III that the weight factors C_{2s} decrease with the increasing of Z . The reason is that the Coulomb attraction between the nucleus and the electrons becomes larger when Z increases, and thus the valence electrons are more likely to stay at the inner shell. Compared with other atoms, the negative ion Li^- exhibits some kind of different characteristics. Unlike the situation for Be or other positive ions, where an electron at a position far from the nucleus will suffer an average Coulomb attraction, the additional electron in Li^- endures no attraction of this kind; therefore, the valence electrons will have a greater possibility of staying at the outer shells. We can see that C_{2s} is only 0.906, much smaller than the values for other ions. This evidence suggests that the present two-configuration model space may be insufficient to describe the behavior of the ground state of Li^- because its valence electrons will have considerable possibilities to appear in outer orbitals.

As has been discussed according to the Z^{-1} expansion theory [27], the correlation energies of Be-like atoms have the following Z dependence:

$$E_c = ZE_1 + E_2 + Z^{-1}E_3 + \dots, \quad (7)$$

where E_1, E_2, E_3, \dots are constants independent of Z . The

TABLE II. Contributions of the second-order diagrams (in 10^{-5} a.u.).

Diagram	Z = 3	Z = 4	Z = 5	Z = 6	Z = 7	Z = 8
$\langle 2s^2 1S H_{\text{eff}} 2s^2 1S \rangle$						
(a),(b)	-3976.1	-4163.7	-4170.2	-4325.6	-4355.5	-4390.8
(c),(d)	-436.0	-780.7	-989.8	-1151.1	-1257.8	-1340.2
(e),(f)	108.1	199.1	257.0	296.2	324.4	345.6
(g)	-5490.6	-4353.3	-4014.0	-3890.5	-3831.2	-3801.6
(h),(i)	-2.7	-10.0	-17.3	-23.5	-28.7	-32.9
(j)	6.8	23.3	38.9	51.8	62.2	70.6
(k)	5.1	17.7	29.9	40.0	48.1	54.8
(l)	-3.8	-12.1	-19.4	-25.3	-29.9	-33.6
Sum	-9789.2	-9079.7	-8884.9	-9028.0	-9068.4	-9128.1
$\langle 2s^2 1S H_{\text{eff}} 2p^2 1S \rangle$						
(g)	5534.0	7361.7	5836.5	5114.3	4676.1	4385.3
(h),(i)	65.4	155.0	209.6	243.7	266.5	282.7
(j)	1.1	5.7	10.5	14.5	17.2	20.3
(k)	9.8	39.1	65.8	86.4	102.2	114.5
(l)	1.4	8.5	17.3	25.1	31.7	37.2
Sum	5611.7	7570.0	6139.7	5484.0	5093.7	4840.0
$\langle 2p^2 1S H_{\text{eff}} 2s^2 1S \rangle$						
(g)	3869.3	4168.7	4025.8	3884.3	3761.4	3664.9
(h),(i)	79.9	212.8	308.2	374.8	423.2	459.7
(j)	1.0	5.3	9.8	13.6	16.6	19.1
(k)	-7.3	-26.9	-43.9	-56.9	-66.8	-74.5
(l)	1.3	8.3	16.8	24.5	31.0	36.5
Sum	3944.2	4368.2	4316.7	4240.3	4165.4	4105.7
$\langle 2p^2 1S H_{\text{eff}} 2p^2 1S \rangle$						
(a),(b)	-3976.1	-4163.7	-4170.2	-4325.6	-4355.5	-4390.8
(c),(d)	-287.7	-842.4	-1256.0	-1565.8	-1784.3	-1951.7
(e),(f)	13.1	50.7	85.3	112.4	133.4	150.0
(g)	-11 397.2	-12 354.4	-12 271.6	-12 209.8	-12 138.7	-12 080.7
(h),(i)	-2.5	-15.8	-33.8	-50.9	-65.7	-78.3
(j)	8.0	55.3	111.0	158.2	195.8	225.9
(k)	3.1	10.0	18.4	25.1	30.3	34.4
(l)	-0.5	-6.0	-15.0	-24.4	-32.9	-40.3
Sum	-15 639.8	-17 266.3	-17 531.9	-17 880.8	-18 017.6	-18 131.5
Diagram	Z = 9	Z = 10	Z = 11	Z = 12	Z = 13	Z = 14
$\langle 2s^2 1S H_{\text{eff}} 2s^2 1S \rangle$						
(a),(b)	-4414.3	-4451.7	-4478.3	-4491.9	-4504.4	-4516.4
(c),(d)	-1404.0	-1458.3	-1502.1	-1537.4	-1567.5	-1593.5
(e),(f)	362.2	375.2	386.0	395.0	402.6	409.1
(g)	-3785.8	-3778.0	-3773.2	-3771.5	-3770.6	-3770.5
(h),(i)	-36.4	-39.4	-41.9	-44.1	-45.9	-47.6
(j)	77.5	83.3	88.2	92.3	95.9	99.1
(k)	60.3	64.9	68.8	72.1	75.0	77.5
(l)	-36.6	-39.1	-41.2	-42.9	-44.5	-45.8
Sum	-9177.1	-9243.1	-9293.7	-9328.4	-9359.4	-9388.1
$\langle 2s^2 1S H_{\text{eff}} 2p^2 1S \rangle$						
(g)	4178.3	4025.0	3905.4	3810.9	3733.4	3669.0
(h),(i)	294.9	304.2	311.7	317.7	322.7	327.0
(j)	22.3	24.0	25.4	26.6	27.7	28.5
(k)	124.3	132.3	138.9	144.4	149.1	153.2
(l)	41.7	45.5	48.8	51.6	54.0	56.1
Sum	4661.5	4531.0	4430.2	4351.2	4286.9	4233.8

TABLE III. (Continued).

Diagram	Z = 9	Z = 10	Z = 11	Z = 12	Z = 13	Z = 14
			$\langle 2p^2\ ^1S H_{\text{eff}} 2s^2\ ^1S \rangle$			
(g)	3588.1	3527.4	3476.3	3434.6	3398.9	3368.3
(h),(i)	488.1	511.0	529.7	545.3	558.5	569.8
(j)	21.1	22.8	24.3	25.5	26.5	27.5
(k)	-80.7	-85.7	-89.9	-93.4	-96.4	-99.0
(l)	41.0	44.8	48.0	50.8	53.3	55.4
Sum	4057.6	4020.3	3988.4	3962.8	3940.8	3922.0
			$\langle 2p^2\ ^1S H_{\text{eff}} 2p^2\ ^1S \rangle$			
(a),(b)	-4414.3	-4451.7	-4478.3	-4491.9	-4504.4	-4516.4
(c),(d)	-2081.2	-2187.0	-2273.6	-2344.6	-2404.7	-2456.4
(e),(f)	163.3	174.2	183.3	190.9	197.5	203.1
(g)	-12033.0	-11996.7	-11964.6	-11938.4	-11915.5	-11895.5
(h),(i)	-89.0	-98.0	-105.7	-112.4	-118.2	-123.3
(j)	250.1	270.1	286.7	300.7	312.6	323.0
(k)	37.7	40.4	42.6	44.4	46.1	47.4
(l)	-46.7	-52.2	-56.9	-61.0	-64.7	-67.8
Sum	-18213.1	-18300.9	-18366.5	-18412.3	-18451.3	-18485.9
Diagram	Z = 15	Z = 16	Z = 17	Z = 18	Z = 19	Z = 20
			$\langle 2s^2\ ^1S H_{\text{eff}} 2s^2\ ^1S \rangle$			
(a),(b)	-4525.7	-4534.0	-4542.7	-4549.1	-4554.9	-4560.0
(c),(d)	-1615.9	-1635.6	-1653.2	-1668.6	-1682.4	-1694.9
(e),(f)	414.8	419.7	424.1	427.9	431.4	434.5
(g)	-3770.9	-3771.7	-3772.5	-3773.5	-3774.6	-3775.6
(h),(i)	-49.0	-50.3	-51.5	-52.5	-53.4	-54.3
(j)	101.8	104.3	106.4	108.4	110.2	111.8
(k)	79.7	81.6	83.4	85.0	86.4	87.6
(l)	-46.9	-48.0	-48.9	-49.7	-50.4	-51.1
Sum	-9412.1	-9434.0	-9454.9	-9472.1	-9487.7	-9502.0
			$\langle 2s^2\ ^1S H_{\text{eff}} 2p^2\ ^1S \rangle$			
(g)	3614.6	3568.2	3528.1	3493.0	3462.1	3434.8
(h),(i)	330.6	333.7	336.4	338.8	340.9	342.8
(j)	29.3	30.0	30.6	31.1	31.6	32.1
(k)	156.7	159.8	162.6	165.0	167.2	169.2
(l)	57.9	59.7	61.0	62.3	63.5	64.6
Sum	4189.1	4151.4	4118.7	4090.2	4065.3	4043.5
			$\langle 2p^2\ ^1S H_{\text{eff}} 2s^2\ ^1S \rangle$			
(g)	3341.6	3318.6	3298.1	3279.9	3263.7	3249.0
(h),(i)	579.6	588.2	595.8	602.5	608.6	614.0
(j)	28.3	29.0	29.6	30.2	30.7	31.2
(k)	-101.3	-103.2	-105.0	-106.6	-108.0	-109.3
(l)	57.3	58.9	60.4	61.7	62.9	64.0
Sum	3905.5	3891.5	3878.9	3867.7	3857.9	3849.0
			$\langle 2p^2\ ^1S H_{\text{eff}} 2p^2\ ^1S \rangle$			
(a),(b)	-4525.7	-4534.0	4542.7	-4549.1	-4554.9	-4560.0
(c),(d)	-2501.0	-2540.1	-2574.6	-2605.1	-2632.5	-2657.0
(e),(f)	208.1	212.4	216.3	219.7	222.8	225.6
(g)	-11878.1	-11863.1	-11849.6	-11837.7	-11826.9	-11817.4
(h),(k)	-127.9	-131.9	-135.4	-138.6	-141.6	-144.2
(j)	332.1	340.1	347.1	353.4	359.0	364.1
(k)	48.6	49.7	50.6	51.4	52.2	52.8
(l)	-70.8	-73.2	-75.5	-77.5	-79.4	-81.0
Sum	-18514.7	-18540.1	-18563.8	-18583.5	-18601.3	-18617.1

TABLE III. (Continued).

Diagram	Z = 21	Z = 22	Z = 23	Z = 24	Z = 25	Z = 26
	$\langle 2s^2 1S H_{\text{eff}} 2s^2 1S \rangle$					
(a),(b)	-4564.7	-4569.0	-4574.4	-4578.0	-4581.6	-4584.5
(c),(d)	-1706.0	-1716.5	-1726.1	-1734.7	-1742.5	-1749.9
(e),(f)	437.7	439.9	442.2	444.4	446.3	448.2
(g)	-3776.6	-3777.6	-3778.5	-3779.5	-3780.5	-3781.4
(h),(i)	-55.1	-55.8	-56.4	-57.0	-57.6	-58.1
(j)	113.2	114.6	115.8	116.9	117.9	118.9
(k)	88.8	89.9	90.9	91.8	92.6	93.4
(l)	-51.7	-52.2	-52.7	-53.2	-53.6	-54.0
Sum	-9514.4	-9526.7	-9539.2	-9549.3	-9559.0	-9567.4
	$\langle 2s^2 1S H_{\text{eff}} 2p^2 1S \rangle$					
(g)	3410.2	3388.1	3368.2	3350.2	3333.9	3318.8
(h),(i)	344.5	346.0	347.4	348.7	349.8	350.9
(j)	32.5	32.8	33.2	33.5	33.8	34.0
(k)	171.0	172.6	174.1	175.5	176.7	177.9
(l)	65.6	66.5	67.3	68.1	68.8	69.4
Sum	4023.8	4006.0	3990.2	3976.0	3963.0	3951.0
	$\langle 2p^2 1S H_{\text{eff}} 2s^2 1S \rangle$					
(g)	3236.0	3223.8	3212.9	3203.0	3193.9	3185.4
(h),(i)	618.9	623.4	627.5	631.2	634.6	637.8
(j)	31.6	32.0	32.3	32.7	33.0	33.3
(k)	-110.4	-111.5	-112.4	-113.3	-114.2	-114.9
(l)	65.0	66.0	66.8	67.6	68.3	69.0
Sum	3841.1	3833.7	3827.1	3821.2	3815.6	3810.6
	$\langle 2p^2 1S H_{\text{eff}} 2p^2 1S \rangle$					
(a),(b)	-4564.7	-4569.0	-4574.4	-4578.0	-4581.6	-4584.5
(c),(d)	-2679.2	-2699.9	-2718.4	-2735.3	-2751.3	-2765.1
(e),(f)	228.2	230.5	232.6	234.5	236.3	238.0
(g)	-11 808.7	-11 800.6	-11 793.4	-11 786.7	-11 780.6	-11 775.1
(h),(i)	-146.6	-148.8	-150.9	-152.8	-154.5	-156.2
(j)	368.7	372.9	376.7	380.3	383.5	386.5
9k)	53.4	54.0	54.5	54.9	55.4	55.8
(l)	-82.6	-84.0	-85.3	-86.5	-87.6	-88.8
Sum	-18 631.5	-18 644.9	-18 658.6	-18 669.6	-18 680.4	-18 689.4
Diagram	Z = 27	Z = 28	Z = 29	Z = 30	Z = 31	Z = 32
	$\langle 2s^2 1S H_{\text{eff}} 2s^2 1S \rangle$					
(a),(b)	-4587.3	-4590.0	-4592.4	-4594.8	-4596.9	-4598.9
(c),(d)	-1756.6	-1762.9	-1768.7	-1774.0	-1779.3	-1784.1
(e),(f)	449.8	451.4	452.9	454.2	455.5	456.7
(g)	-3782.3	-3783.1	-3783.9	-3784.7	-3785.4	-3786.1
(h),(i)	-58.6	-59.0	-59.4	-59.8	-60.2	-60.5
(j)	119.8	120.6	121.4	122.1	122.8	123.5
(k)	94.1	94.8	95.4	96.0	96.5	97.0
(l)	-54.4	-54.7	-55.0	-55.3	-55.6	-55.9
Sum	-9575.5	-9582.9	-9589.7	-9596.3	-9602.6	-9608.3
	$\langle 2s^2 1S H_{\text{eff}} 2p^2 1S \rangle$					
(g)	3305.0	3292.3	3280.5	3269.5	3259.4	3249.9
(h),(i)	351.9	352.8	353.6	354.4	355.1	355.8
(j)	34.3	34.5	34.7	34.9	35.1	35.2
(k)	179.0	180.0	180.9	181.8	182.6	183.3
(l)	70.0	70.6	71.1	71.6	72.1	72.5
Sum	3940.2	3930.2	3920.8	3912.2	3904.3	3896.7

TABLE III. (Continued).

Diagram	Z = 27	Z = 28	Z = 29	Z = 30	Z = 31	Z = 32
			$\langle 2p^2\ ^1S H_{\text{eff}} 2s^2\ ^1S \rangle$			
(g)	3177.6	3170.4	3163.7	3157.4	3151.6	3146.1
(h),(i)	640.7	643.5	646.0	648.4	650.6	652.7
(j)	33.5	33.8	34.0	34.2	34.4	34.6
(k)	-115.6	-116.3	-116.9	-117.4	-118.0	-118.5
(l)	69.6	70.1	70.7	71.2	71.7	72.1
Sum	3805.8	3801.5	3797.5	3793.8	3790.3	3787.0
			$\langle 2p^2\ ^1S H_{\text{eff}} 2p^2\ ^1S \rangle$			
(a),(b)	-4587.3	-4590.0	-4592.4	-4594.8	-4596.9	-4598.9
(c),(d)	-2778.3	-2790.6	-2802.0	-2812.4	-2822.6	-2831.9
(e),(f)	239.5	241.0	242.3	243.7	244.7	245.8
(g)	-11 770.0	-11 764.5	-11 760.6	-11 756.6	-11 752.6	-11 748.9
(h),(i)	-157.7	-159.1	-160.3	-161.6	-162.7	-163.9
(j)	389.3	391.9	394.4	396.6	398.7	400.6
(k)	56.2	56.5	56.8	57.1	57.4	57.7
(l)	-89.7	-90.6	-91.5	-92.2	-92.9	-93.6
Sum	-18 698.0	-18 705.4	-18 713.3	-18 720.2	-18 726.9	-18 733.1
Diagram	Z = 33	Z = 34	Z = 35	Z = 36		
			$\langle 2s^2\ ^1S H_{\text{eff}} 2s^2\ ^1S \rangle$			
(a),(b)	-4600.7	-4602.8	-4604.5	-4606.0		
(c),(d)	-1788.5	-1792.8	-1796.8	-1800.6		
(e),(f)	457.8	458.9	459.8	460.8		
(g)	-3786.8	-3787.6	-3788.2	-3788.8		
(h),(i)	-60.9	-61.2	-61.5	-61.7		
(j)	124.1	124.6	125.2	125.7		
(k)	97.5	98.0	98.4	98.8		
(l)	-56.1	-56.3	-56.6	-56.8		
Sum	-9613.6	-9619.2	-9624.2	-9628.6		
			$\langle 2s^2\ ^1S H_{\text{eff}} 2p^2\ ^1S \rangle$			
(g)	3241.1	3232.9	3225.2	3217.8		
(h),(i)	356.5	357.1	357.6	358.1		
(j)	35.4	35.6	35.7	35.8		
(k)	184.1	184.7	185.4	186.0		
(l)	72.9	73.3	73.6	74.0		
Sum	3890.0	3883.6	3877.5	3871.7		
			$\langle 2p^2\ ^1S H_{\text{eff}} 2s^2\ ^1S \rangle$			
(g)	3141.0	3136.3	3131.8	3127.4		
(h),(i)	654.6	656.5	658.2	659.9		
(j)	34.8	34.9	35.1	35.2		
(k)	-118.9	-119.4	-119.8	-120.2		
(l)	72.5	72.9	73.3	73.6		
Sum	3784.0	3781.2	3778.6	3775.9		
			$\langle 2p^2\ ^1S H_{\text{eff}} 2p^2\ ^1S \rangle$			
(a),(b)	-4600.7	-4602.8	-4604.5	-4606.0		
(c),(d)	-2840.7	-2849.0	-2856.7	-2864.1		
(e),(f)	246.9	247.8	248.7	249.6		
(g)	-11 745.5	-11 742.5	-11 739.5	-11 736.7		
(h),(i)	-164.9	-165.8	-166.7	-167.7		
(j)	402.5	404.3	405.9	407.5		
(k)	57.9	58.1	58.4	58.6		
(l)	-94.3	-94.8	-95.5	-96.0		
Sum	-18 738.8	-18 744.7	-18 749.9	-18 754.7		

TABLE III. Comparison of the second-order MBPT results of correlation energies and the experimental values (in a.u.).

Z	E_{HF}	E_{total}	C_{2s}	E_c^{theor}	$E_c^{\text{expt a}}$	ΔE_c	$E_c^{\text{theor}}/E_c^{\text{expt}}$
3	-7.428 23	-7.502 42	0.906	0.074 19	0.0722 ^b	-0.0020	102.8%
4	-14.573 02	-14.660 94	0.942	0.087 92	0.094 34	0.0064	93.2%
5	-24.237 58	-24.344 73	0.958	0.1072	0.1114	0.0042	96.1%
6	-36.408 50	-36.532 97	0.959	0.1245	0.1264	0.0019	98.5%
7	-51.082 32	-51.221 26	0.965	0.1389	0.1405	0.0016	98.9%
8	-68.257 71	-68.410 46	0.967	0.1528	0.1540	0.0012	99.2%
9	-87.934 05	-88.100 04	0.969	0.1660	0.1671	0.0011	99.3%
10	-110.111 01	-110.290 11	0.969	0.1791	0.1799	0.0008	99.6%
11	-134.788 40	-134.980 27	0.969	0.1919	0.1925	0.0006	99.7%
12	-161.966 08	-162.170 47	0.970	0.2044	0.2050	0.0006	99.7%
13	-191.644 00	-191.860 75	0.971	0.2168	0.2174	0.0006	99.7%
14	-223.822 08	-224.051 14	0.971	0.2291	0.2296	0.0005	99.8%
15	-258.500 30	-258.741 56	0.971	0.2413	0.2418	0.0005	99.8%
16	-295.678 63	-295.932 03	0.971	0.2534	0.2540	0.0006	99.8%
17	-335.357 04	-335.622 54	0.971	0.2655	0.2660	0.0005	99.8%
18	-377.535 52	-377.813 07	0.972	0.2776	0.2781	0.0005	99.8%
19	-422.214 07	-422.503 63	0.972	0.2896	0.2901	0.0005	99.8%
20	-469.392 66	-469.694 19	0.972	0.3015	0.3021	0.0006	99.8%
21	-519.071 29	-519.384 78	0.972	0.3135			
22	-571.249 96	-571.575 39	0.972	0.3254			
23	-625.928 65	-626.266 02	0.972	0.3374			
24	-683.107 38	-683.456 64	0.972	0.3493			
25	-742.786 13	-743.147 28	0.972	0.3612			
26	-804.964 90	-805.337 92	0.972	0.3730			
27	-869.643 68	-870.028 56	0.973	0.3849			
28	-936.822 48	-937.219 21	0.973	0.3967			
29	-1006.501 30	-1006.909 87	0.973	0.4086			
30	-1078.680 13	-1079.100 53	0.973	0.4204			
31	-1153.358 97	-1153.791 21	0.973	0.4322			
32	-1230.537 82	-1230.981 88	0.973	0.4441			
33	-1310.216 68	-1310.672 55	0.973	0.4559			
34	-1392.395 55	-1392.863 23	0.973	0.4677			
35	-1477.074 43	-1477.553 89	0.973	0.4795			
36	-1564.253 31	-1564.744 60	0.973	0.4913			

^aReference [22].

^bReference [25].

first term in Eq. (7) comes from the degeneracy of the $2s$ and $2p$ orbitals in the zero-order Z^{-1} expansion. Thus an approximation that incorporates the $2s$ and $2p$ configuration into the zero-order wave function should be able to produce this linear dependence of Z . In the present calculation, the $2s$ and $2p$ orbitals are all included in the model space; therefore, the first-order MBPT results have included the contribution of the first term of Eq. (7). Higher-order perturbation corrections contribute mainly to the latter terms in Eq. (7). The calculated correlation energies can also be expanded in the Z^{-1} series

$$E'_c = ZE_1 + E'_2 + Z^{-1}E'_3 + \dots \quad (8)$$

The discrepancy of the experimental values from the present calculation satisfies the following relation

$$\Delta E_c = \Delta E_2 + Z^{-1}\Delta E_3 + \dots \quad (9)$$

It is clear from Eq. (9) that ΔE_c approaches a constant while Z increases. In the seventh column in Table III, we give the differences of the experimental values and the second-order MBPT results, which give a constant value of about 0.0005 for large Z values. Based on this fact, the correlation energies for ions with $Z > 20$, whose accurate experimental values are still not available, can be obtained with high accuracy by adding this constant to our MBPT results listed in Table III.

ACKNOWLEDGMENT

This work is supported by the National Natural Science Foundation of China and Grant No. LWTZ-1298 of Chinese Academy of Sciences.

- [1] H. P. Kelly, Phys. Rev. **131**, 684 (1963); **136**, B896 (1964); **173**, 142 (1968); **180**, 55 (1969).
 [2] E. S. Chang, R. T. Pu, and T. D. Das, Phys. Rev. **174**, 1 (1968).

- [3] I. Lindgren, Phys. Rev. A **31**, 1273 (1985).
 [4] Jinhua Xi, Lijin Wu, Baiwen Li, and Jiangyong Wang, Phys. Lett. A **152**, 401 (1991).
 [5] Jinhua Xi and Lijin Wu, Acta Phys. Sin. **41**, 370 (1992) (in

- Chinese).
- [6] S. Wilson and D. M. Silver, *Phys. Rev. A* **14**, 1949 (1976).
- [7] S. Salomonson and P. Öster, *Phys. Rev. A* **40**, 5548 (1989); *A* **40**, 5559 (1989).
- [8] W. R. Johnson and J. Sapirstein, *Phys. Rev. Lett.* **57**, 1126 (1986).
- [9] W. R. Johnson, S. A. Blundell, and J. Sapirstein, *Phys. Rev. A* **37**, 307 (1988); **42**, 1087 (1990).
- [10] C. F. Fischer and W. Guo, *J. Comp. Phys.* **90**, 486 (1990).
- [11] C. F. Fischer, in *Proceedings of the 12th International Conference on Atomic Physics*, Post Abstracts, VII-I, edited by W. E. Baylis, G. W. F. Drake, and J. W. McConkey (University of Michigan, Ann Arbor, 1990).
- [12] C. F. Fischer and M. Idrees, *Comp. Phys.* **3**, 53 (1989); *J. Phys. B* **23**, 679 (1990).
- [13] T. N. Chang, *Phys. Rev. A* **39**, 4946 (1989).
- [14] T. N. Chang and X. Tang, *Phys. Rev. A* **44**, 232 (1991).
- [15] Jinhua Xi and Lijin Wu, *Acta Phys. Sin.* **41**, 1759 (1992) (in Chinese).
- [16] Jinhua Xi, Lijin Wu, and Baiwen Li, *Acta Phys. Sin.* (to be published) (in Chinese).
- [17] Jinhua Xi, Lijin Wu, Xinghong He, and Baiwen Li, *Phys. Rev. A* **46**, 5806 (1992).
- [18] Wenyu Liu, Jinhua Xi, Xinghong He, Lijin Wu, and Baiwen Li, *Phys. Rev. A* (to be published).
- [19] G. A. Petersson and Stuart L. Licht, *J. Chem. Phys.* **75**, 4556 (1981).
- [20] S. Shankar and P. T. Narasimhan, *Phys. Rev. A* **29**, 58 (1984).
- [21] Baiwen Li, R. Goldflam, E. Henley, and L. Wilets, *J. Phys. B* **17**, 1445 (1984).
- [22] E. R. Davidson, S. A. Hagstrom, S. J. Chakravorty, V. M. Umar, and C. F. Fischer, *Phys. Rev. A* **44**, 7071 (1991).
- [23] C. deBoor, *A Practical Guide to Splines* (Springer, New York, 1978).
- [24] I. Lindgren and J. Morrison, *Atomic Many-Body Theory* (Springer-Verlag, Berlin, 1982).
- [25] J. S. Sims, S. A. Hagstrom, D. Munch, and C. F. Bunge, *Phys. Rev. A* **13**, 560 (1976).
- [26] S. Salomonson, I. Lindgren, and A-M. Martensson, *Phys. Scr.* **21**, 351 (1980).
- [27] A. Hibbert, *Rep. Prog. Phys.* **38**, 1217 (1975).